

Peptide–lipid interactions of the β -hairpin antimicrobial peptide tachyplesin and its linear derivatives from solid-state NMR

Timothy Doherty^a, Alan J. Waring^b, Mei Hong^{a,*}

^a Department of Chemistry, Iowa State University, Ames, IA 50011, USA

^b Department of Medicine, University of California at Los Angeles School of Medicine, Los Angeles, CA 90095, USA

Received 29 November 2005; received in revised form 13 March 2006; accepted 14 March 2006

Available online 5 April 2006

Abstract

The peptide–lipid interaction of a β -hairpin antimicrobial peptide tachyplesin-1 (TP-1) and its linear derivatives are investigated to gain insight into the mechanism of antimicrobial activity. ³¹P and ²H NMR spectra of uniaxially aligned lipid bilayers of varying compositions and peptide concentrations are measured to determine the peptide-induced orientational disorder and the selectivity of membrane disruption by tachyplesin. The disulfide-linked TP-1 does not cause any disorder to the neutral POPC and POPC/cholesterol membranes but induces both micellization and random orientation distribution to the anionic POPE/POPG membranes above a peptide concentration of 2%. In comparison, the anionic POPC/POPG bilayer is completely unaffected by TP-1 binding, suggesting that TP-1 induces negative curvature strain to the membrane as a mechanism of its action. Removal of the disulfide bonds by substitution of Cys residues with Tyr and Ala abolishes the micellization of POPE/POPG bilayers but retains the orientation randomization of both POPC/POPG and POPE/POPG bilayers. Thus, linear tachyplesin derivatives have membrane disruptive abilities but use different mechanisms from the wild-type peptide. The different lipid–peptide interactions between TP-1 and other β -hairpin antimicrobial peptides are discussed in terms of their molecular structure. © 2006 Elsevier B.V. All rights reserved.

Keywords: Antimicrobial peptide; Tachyplesin; β -hairpin; Membrane disruption; Lipid bilayer; Solid-state NMR

1. Introduction

One of the approaches for understanding the structure–activity relationship of membrane destructive antimicrobial peptides is to investigate the molecular interaction between the peptide and the lipids using solid-state NMR spectroscopy. The peptide–lipid interaction can be examined as a function of both the amino acid sequence and the membrane composition, to address questions such as the importance of structural amphiphilicity and charge distribution to membrane disruption, and how membrane components such as cholesterol and anionic lipids modulate the peptide–lipid interaction. ³¹P and ²H NMR are ideal probes for the peptide–lipid interactions. The ³¹P chemical shift tensor interaction is exquisitely sensitive to the lipid headgroup conformation,

lipid phase, and electrostatic perturbation to the membrane surface [1]. ²H quadrupolar couplings complement ³¹P NMR by providing information on the lipid chain dynamics and thus the fluidity of the hydrophobic part of the membrane. These experiments are best conducted on uniaxially aligned membranes to resolve the signals of non-bilayer lipids that are often induced by the peptides [2,3]. A number of antimicrobial peptides have been investigated using this uniaxial alignment NMR approach [4–9].

One class of antimicrobial peptides is characterized by disulfide-stabilized β -sheet conformation, of which protegrin-1 (PG-1) and tachyplesin-1 (TP-1) are two well-studied examples. Both exhibit potent and broad-spectrum activities against Gram-positive and Gram-negative bacteria, fungi, and some viruses [10,11]. Both peptides contain two cross-strand disulfide bonds and six cationic residues. However, the distribution of the charged residues differs: PG-1 has the Arg residues located at the two long ends of the β -hairpin, leaving the central part of the molecule hydrophobic, while TP-1 has the Arg residues distributed throughout the sequence (Fig. 1). ¹H solution NMR studies confirmed that both peptides adopt a well-defined β -hairpin structure

Abbreviations: TP-1, tachyplesin; PG-1, protegrin-1; POPE, 1-palmitoyl-2-oleoyl-*sn*-glycero-3-phosphatidylethanolamine; POPC, 1-palmitoyl-2-oleoyl-*sn*-glycero-3-phosphatidylcholine; POPG, 1-palmitoyl-2-oleoyl-*sn*-glycero-3-phosphatidylglycerol; PA, phosphatidic acid

* Corresponding author. Tel.: +1 515 294 3521; fax: +1 515 294 0105.

E-mail address: mhong@iastate.edu (M. Hong).

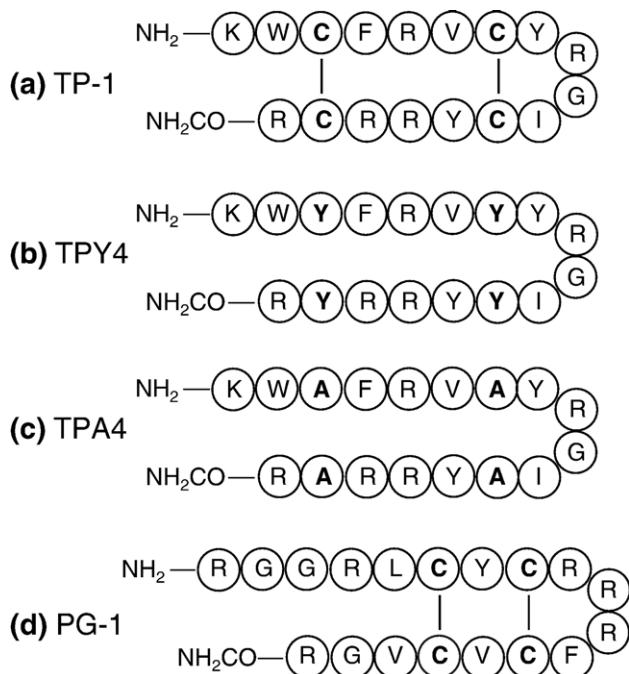


Fig. 1. Amino acid sequence of (a) TP-1, (b) TPY4, (c) TPA4, and (d) PG-1.

in aqueous solution [12,13]. However, when bound to DPC micelles, the TP-1 β -hairpin is reported to undergo a significant conformational rearrangement and bends around the middle of the two strands, incurring a significant curvature [14].

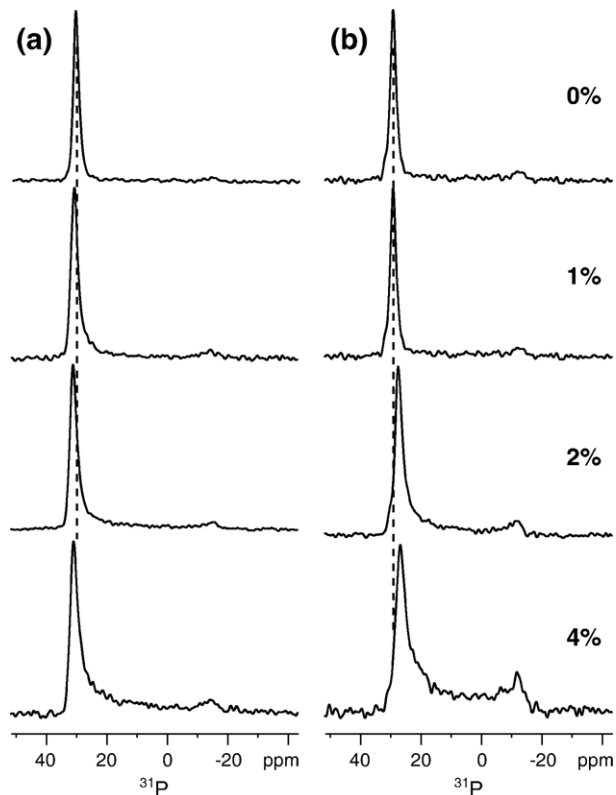


Fig. 2. ³¹P spectra of uniaxially aligned (a) POPC and (b) POPC:cholesterol (3:1) bilayers in the presence of TP-1. Peptide concentrations are 0, 1%, 2%, and 4%. Dashed lines guide the eye for the 0° frequency peaks.

In addition to wild-type PG-1 and TP-1, derivatives of both peptides have been examined to gain insight into the sequence determinants of antimicrobial activity. We studied the peptide–lipid interactions of two PG-1 mutants: in one mutant the disulfide bonds are removed by Cys→Ala mutation, while in the other mutant the number of cationic residues is reduced from six to three [15]. ³¹P NMR spectra showed that the Ala mutant nearly completely lost its membrane-disruptive ability while the charge-reduced mutant caused significant membrane perturbation [15]. These are consistent with the activities of the peptides [16]. Moreover, ¹H solution NMR spectra indicate that the Ala mutant is a random coil in solution while the charge-reduced PG-1 mutant maintains a β -hairpin fold. For TP-1, Cys→Ala mutation (TPA4) similarly caused the peptide to become a random coil in solution based on circular dichroism experiments, while Cys→Tyr substitution (TPY4) retained the β -hairpin fold through π – π stacking interactions based on ¹H NMR spectra [14]. Again, these solution conformations correlate well with the antimicrobial activities: TPA4 is inactive while TPY4 has strong antibacterial and antifungal activities [17].

In this study, we use ³¹P and ²H solid-state NMR to investigate the interactions of TP-1 and its Ala and Tyr derivatives with lipid bilayers of varying compositions. We assess the membrane-

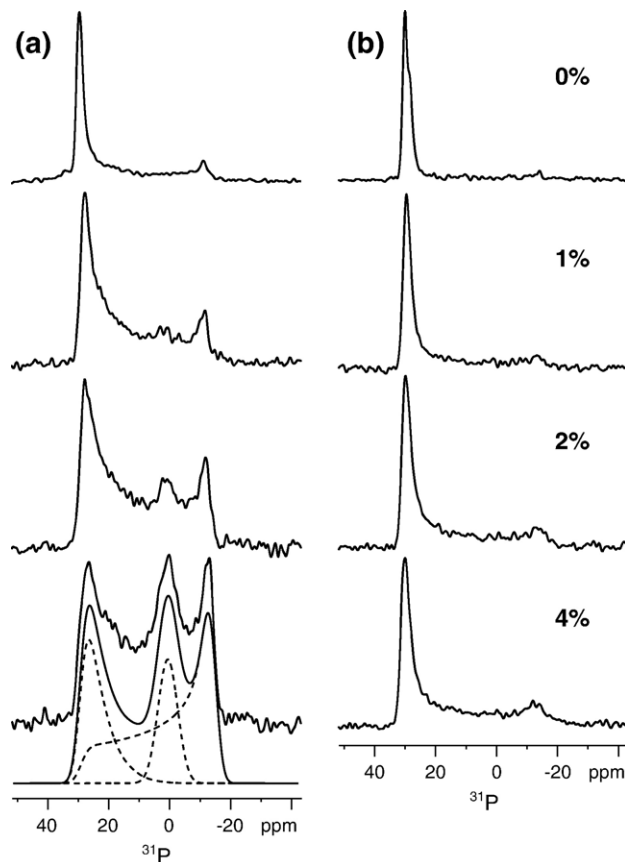


Fig. 3. ³¹P spectra of uniaxially aligned (a) POPE : POPG (3:1) and (b) POPC : POPG (3:1) bilayers in the presence of TP-1. Peptide concentrations are 0, 1%, 2%, and 4%. The POPE/POPG spectrum with 4% TP-1 is best fit with a combination of a residual oriented peak (27%), an isotropic peak (18%), and a uniaxial powder lineshape (55%). The individual components are shown as dashed lines.

disruptive abilities of these peptides through non-bilayer intensities and unoriented powder intensities in the spectra of uniaxially aligned lipids. Interestingly, the tachyplesin peptides show several important differences from the protegrins in their membrane-interaction profiles, and the linear derivatives of TP-1 cause comparable or stronger membrane perturbation compared to wild-type TP-1. The implications of these differences will be discussed.

2. Materials and methods

2.1. Preparation of uniaxially aligned membranes

All lipids were purchased from Avanti Polar Lipids (Alabaster, AL) and used without further purification. TP-1, TPA4, and TPY4 were synthesized using Fmoc solid-phase peptide synthesis protocols. The amino acid sequences of the three tachyplesins are shown in Fig. 1 and compared to the sequence of PG-1.

Glass-plate orientated membranes were prepared using a naphthalene-incorporated procedure [18]. The peptide was dissolved in TFE and mixed with a chloroform solution of the desired amount of lipids. The mixture was dried under a stream of N_2 gas and the dried film was redissolved in a 2:1 mixture of chloroform/TFE containing a three-fold excess of naphthalene with respect to the lipids. The solution was deposited on glass plates (Marienfeld Laboratory Glassware) of ~ 80 μm thickness and 6×12 mm^2 size at a density of ~ 0.01 mg/mm^2 . The sample was air dried for 2 h and then vacuum dried overnight to remove all the solvents and naphthalene. The dried membranes were hydrated first by direct deposition of ~ 1 μL water per plate, and then through vapor diffusion at 98% relative humidity over a saturated solution of K_2SO_4 for 3–5 days at room temperature. Subsequently, the glass plates were stacked, wrapped in parafilm and sealed in a polyethylene bag to prevent dehydration. To ensure reproducibility, all membrane series as a function of peptide concentration were repeated multiple times. Peptide–lipid molar ratios of 0, 1:100, 1:50, and 1:25 were used and were denoted as concentrations of 0, 1%, 2%, and 4%, respectively.

2.2. Solid-state NMR experiments

NMR experiments were conducted on a Bruker DSX-400 spectrometer operating at a resonance frequency of 162.12 MHz for ^{31}P and 400.49 MHz for ^1H . ^{31}P spectra of oriented peptide–lipid mixtures were collected using a double-resonance probe equipped with a custom-designed radio-frequency coil with a rectangular cross section and a dimension of $12 \times 6 \times 5$ mm (L \times W \times H). The samples were inserted into the magnet with the alignment axis parallel to the external magnetic field B_0 . The ^{31}P chemical shift was referenced externally to 85% phosphoric acid at 0 ppm. A typical ^{31}P 90° pulse length of 5 μs , a ^1H decoupling field strength of 50 kHz, and a recycle delay of 2 s were used. Experiments on oriented membranes were conducted between 291 K and 300 K, above the phase transition temperatures of the POPC and POPG lipids (271 K) and the estimated phase transition temperature of the POPE/POPG membrane (291 K). ^2H spectra of the POPE/ d_{31} -POPG membrane were collected at 300 K using a standard quadrupolar echo sequence. Magic-angle spinning (MAS) experiments on POPE/POPG membrane samples were carried out on a triple-resonance MAS probe with a 4-mm spinning module.

3. Results

3.1. Lipid–peptide interaction of wild-type TP-1

We first examine the interaction of wild-type TP-1 with zwitterionic phosphatidylcholine (PC) membranes. Fig. 2 shows representative ^{31}P spectra of uniaxially aligned POPC and POPC/cholesterol bilayers containing 0–4% TP-1. If no orientational disorder is present, a single peak at ~ 30 ppm, corresponding to the 0° edge of the ^{31}P chemical shift anisotropy (CSA) powder pattern, is expected due to the parallel orientation of the bilayer normal with respect to B_0 . Any peptide-induced membrane disorder is manifested as intensities away from this 0°

frequency. Fig. 2 shows that TP-1 creates minimal disorder in either neutral membranes even at the highest peptide concentration used, as little intensity is observed away from the 0° peak. While other antimicrobial peptides such as RTD-1 and PG-1 can also preserve the orientational order of cholesterol-containing phosphatidylcholine membranes [6,19], the complete retention of the orientational order of pure POPC bilayers by TP-1 is more unexpected: for example, PG-1 completely disrupts the POPC bilayer structure above a concentration of 3%. TP-1 also causes a small reduction of the ^{31}P chemical shift anisotropy in POPC/cholesterol membranes, as shown by an upfield shift of the 0° frequency peak with increasing concentrations of the peptide. Since the spectral linewidth is little affected by the peptide, this suggests a small conformational change of the lipid headgroup upon TP-1 binding.

While neutral and cholesterol-containing bilayers mimic the composition of mammalian cell membranes, bacterial membranes contain significant amounts of anionic lipids, which better attract the cationic antimicrobial peptides [20]. Thus, we investigated the interaction of TP-1 with two anionic bilayers, POPE/POPG (3:1) and POPC/POPG (3:1), where the difference is the headgroup size of the zwitterionic lipid component. Fig. 3 shows representative ^{31}P spectra of these two membranes with varying concentrations of TP-1. A dramatic difference is observed: the addition of TP-1 had almost no effect on the structure of the POPC/POPG bilayers (Fig. 3b), but creates a significant 90° peak at -12 ppm and an isotropic peak near 0 ppm in the POPE/POPG spectra (Fig. 3a). The 90° peak and the broad low intensities in the entire CSA range indicate that a significant fraction of the lamellar bilayers has become randomly oriented instead of uniaxially aligned as a result of TP-1 binding. The isotropic peak, on the other hand, indicates the formation of non-bilayer micelles or small vesicles. The broadness of the isotropic peak indicates that these vesicles are not so small as to undergo fast isotropic tumbling on timescales shorter than the inverse of the ^{31}P chemical shift anisotropy.

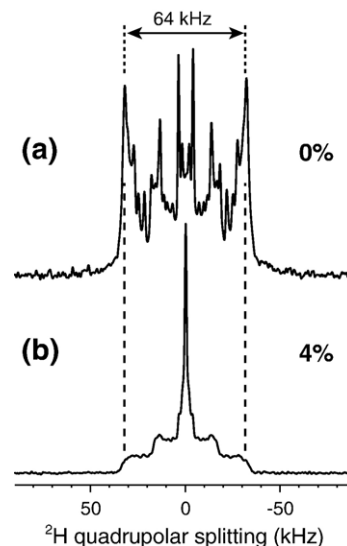


Fig. 4. ^2H spectra of anionic POPE : d_{31} -POPG (3:1) bilayers (a) without TP-1 and (b) with 4% TP-1. Dashed lines guide the eye for the largest quadrupolar splitting.

Spectral simulation for the 4% peptide bound POPE/POPG sample gives the percentages of the three lipid components: the residual oriented bilayers with a mosaic spread of 35° (27%); the isotropic vesicles (18%), and the randomly oriented bilayers (55%). The fact that these disorders are conspicuously absent in the POPC/POPG spectra indicates that TP-1 action is extremely sensitive to the curvature of the lipid bilayer: membrane disruption is strongly facilitated by the negative curvature of POPE-containing bilayer, while the larger POPC headgroup counters this effect, thus maintaining the bilayer order in the presence of the peptide.

To determine the dynamics of the hydrophobic part of the POPE/POPG membrane at high concentrations of TP-1, we incorporated *sn-1* chain perdeuterated d_{31} -POPG lipids into the mixture and measured its ^2H spectra in the absence and presence of TP-1. Fig. 4 compares the resulting spectra. The control sample shows well resolved splittings corresponding to the different motional order parameters along the acyl chain: the more rigid groups near the glycerol backbone give rise to larger quadrupolar splittings while the more mobile groups near the

chain termini produce smaller splittings. The maximum splitting is 64 kHz, corresponding to a $\text{C}-^2\text{H}$ order parameter of 0.26. The addition of TP-1 significantly broadened the spectra to the point where the splittings are no longer resolved; however, the coupling strengths remain unaffected, as seen, for example, in the maximum splitting (Fig. 4). Thus, TP-1 binding does not cause lateral expansion of the bilayer, which would reduce the acyl-chain order parameters. The ^2H spectrum also has a zero-frequency peak, consistent with the isotropic peak in the ^{31}P spectrum (Fig. 3a) that is attributed to small vesicle formation.

To identify whether the cationic TP-1 selectively binds to the anionic POPG lipids to create the isotropic vesicles, we measured the ^{31}P MAS spectra of the mixture in the absence and presence of TP-1 (Fig. 5). If the peptide selectively disrupts POPG lipids but not POPE lipids, then preferential broadening or chemical shift changes of the POPG signal but not the POPE peak would be expected. In the absence of TP-1, the POPE and POPG ^{31}P chemical shifts are resolved by 0.5 ppm (with full width at half maximum of 0.25 ppm) in the MAS spectrum (Fig. 5a). Simulation of the MAS sideband intensities and comparison

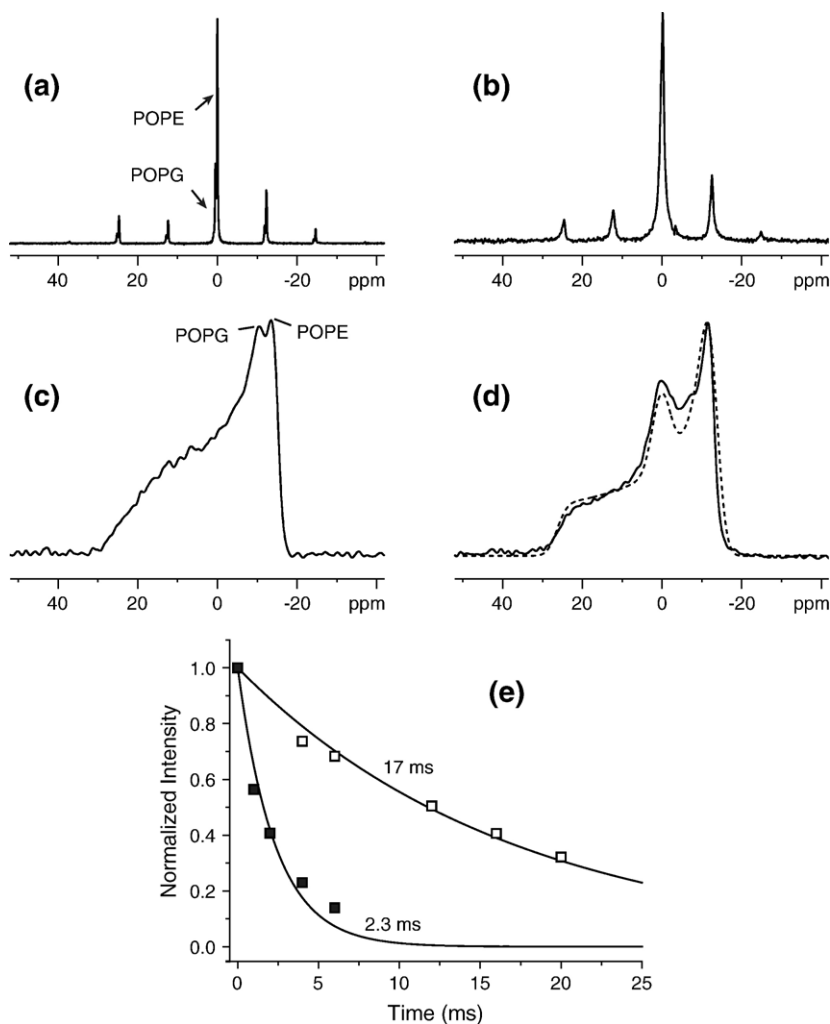


Fig. 5. ^{31}P MAS spectra of unoriented POPE : POPG (3:1) membrane in the absence (a) and presence (b) of 4% TP-1. The corresponding static spectra are shown in (c, d). In (d), the TP-1-bound POPE/POPG ^{31}P spectrum is best fit (dashed line) by a combination of 10% of an isotropic peak and 90% of a uniaxial powder lineshape. (e) ^{31}P Hahn echo intensities as a function of echo delay time for POPE/POPG lipids with 4% TP-1 (filled squares) and for POPE lipids without TP-1 (open squares). The decay constant, T_2 , is much shorter for the peptide-bound membrane (2.3 ms) than for the pure lipid (17 ms).

with the static powder lineshapes of the mixed membrane (Fig. 5c) and of the individual lipids (spectra not shown) yield a ^{31}P chemical shift anisotropy parameter, $\delta \equiv \delta_{zz} - \delta_{\text{iso}}$, of 25.3 ppm for POPG and 28.6 ppm for POPE. Upon TP-1 binding, the two peaks in the MAS spectrum broaden to a combined linewidth of 1.2 ppm and become unresolved, while the sideband intensity distribution remains unaffected (Fig. 5b). Since POPG accounts for only 25% of the lipid in the sample, if it is the only component broadened by TP-1, we would expect a noticeably narrower and higher peak for the major lipid component (POPE) that is resolvable from the POPG signal. Instead, both the linewidth and the chemical shift anisotropy indicate that there is no detectable preferential binding of TP-1 to POPG, suggesting that the two lipids are well mixed on the nanometer scale and both are disordered by the peptide. The static ^{31}P spectrum of the peptide-bound POPE/POPG bilayer exhibits a uniaxial powder lineshape superimposed with an isotropic peak at $\sim 10\%$ of the total intensity (Fig. 5d), consistent with the oriented-membrane result. ^{31}P Hahn-echo experiments showed that the TP-1-bound POPE/POPG membrane has a much shorter ^{31}P spin–spin relaxation time (T_2) of 2.3 ms compared to the non-peptide-containing POPE lipids, which has a T_2 of 17 ms (Fig. 5e). These indicate that the line broadening seen in the ^{31}P MAS spectrum is homogeneous in origin, caused by lipid motions on the time scale of the inverse of the ^{31}P chemical shift anisotropy, ~ 200 s.

3.2. Lipid–peptide interaction of TPY4 and TPA4

To understand the role of the disulfide bonds in tachyplesin–membrane interaction, we studied two TP-1 mutants where the Cys residues are replaced by Tyr and Ala. Fig. 6 shows the ^{31}P

spectra of uniaxially aligned POPE/POPG membranes after TPY4 and TPA4 binding and compare these with TP-1. Both mutants lack the isotropic peak of TP-1, but retain the broad intensity distribution that is indicative of unoriented bilayers. Thus, TPY4 and TPA4 randomize the membrane orientations but do not micellize the POPE/POPG bilayers. The intensity difference between TPY4 and TPA4 at the 90° frequency (-12 ppm) is within experimental uncertainty, indicating that the membrane disruptive abilities of the two mutants are similar. Remarkably, unlike TP-1, TPY4 and TPA4 are also highly effective in disrupting the POPC/POPG bilayer: the ^{31}P spectra (Fig. 7) show significant powder intensities similar to those of POPE/POPG bilayers. Thus, TPY4 and TPA4 are more potent in disrupting the POPC/POPG bilayers than the wild-type TP-1, and have little selectivity between POPC/POPG bilayers and POPE/POPG bilayers.

4. Discussion

The ^{31}P NMR spectra reveal several surprising aspects of tachyplesin–lipid interactions that differ from the analogous β -hairpin peptides PG-1 and RTD-1. First, wild-type TP-1 is extremely selective in its membrane perturbation. Among the four lipid compositions examined, POPC, POPC/cholesterol, POPC/POPG, and POPE/POPG, only the POPE/POPG bilayers are disrupted by TP-1 while the other membranes retain their orientational order. The TP-1-induced POPE/POPG membrane disorder includes randomization of the bilayer orientation and the formation of micelles or small vesicles that undergo isotropic tumbling on the intermediate time scale. The latter is likely the main cause of the significantly shorter ^{31}P T_2 relaxation time upon TP-1 binding. Based on the broadening of both the POPE

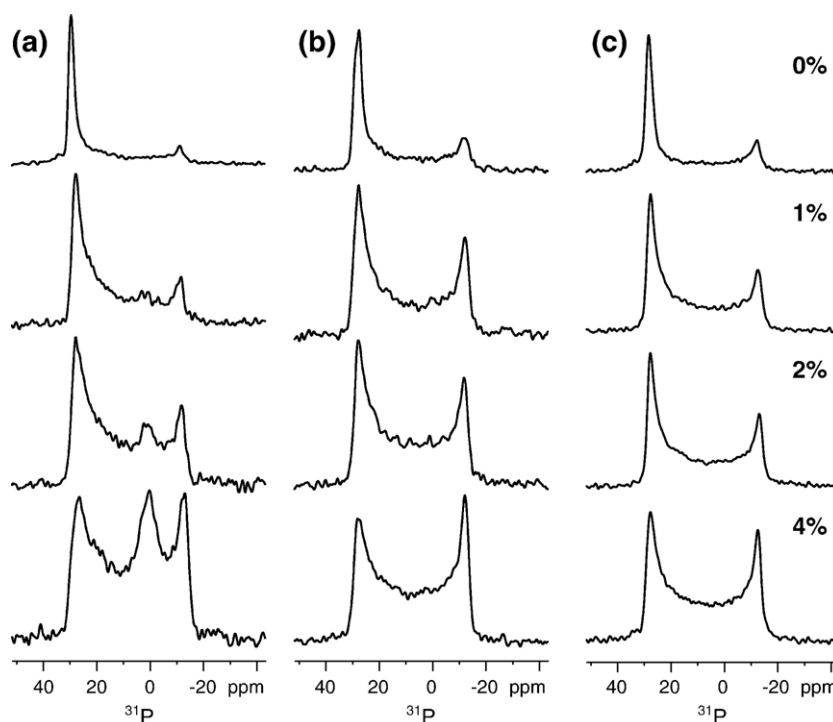


Fig. 6. ^{31}P spectra of uniaxially aligned POPE : POPG (3:1) bilayers in the presence of TP-1 and its linear derivatives. (a) TP-1. (b) TPY4. (c) TPA4. Peptide concentrations are 0, 1%, 2%, and 4%.

and POPG peaks in the ^{31}P MAS spectra, it appears that TP-1 does not exclusively target the anionic POPG lipids and the two lipids are well mixed on the nanometer scale in the membrane.

Since the zwitterionic lipid of bacterial membranes is almost exclusively phosphatidylethanolamine (PE) rather than PC [20], the selective disruption of POPE/POPG membrane by TP-1 is consistent with the peptide's activity profile [11]. The observed micellization of POPE/POPG bilayers is consistent with negative-stain electron microscopy of TP-1 bound to phosphatidylglycerol (PG) lipids and light scattering results on PG bilayers and mixed PE/PG bilayers containing high concentrations (4–20%) of TP-1 [21,22].

The membrane interaction profile of TP-1 differs markedly from that of PG-1 and RTD-1, two other disulfide-linked β -sheet antimicrobial peptides. PG-1 and RTD-1 show strong perturbation of both PC/PG and PE/PG membranes [6,15]. Moreover, PG-1 micellizes PC/PG bilayers but not PE/PG bilayers [15], in contrast to the TP-1 behavior. Given the smaller headgroup of PE compared to PC, this suggests that PG-1 disrupts lipid bilayers through positive curvature strain while TP-1 induces negative curvature strain. The exact molecular mechanism for the opposite curvature strains of the two peptides is not yet known. One possibility is that the membrane-bound TP-1 adopts a conformation that favors negative curvature strain. ^1H solution NMR spectra of TP-1 in DPC micelles indicate that the peptide undergoes a significant conformational rearrangement from the aqueous structure: the backbone of the two strands bends around Arg5 and Arg14, thus increasing the hydrophobic accessible surface area [14]. If this conformational change persists in the bilayer, then it may increase the peptide volume in the hydrophobic region of the bilayer than at the lipid–water interface,

thus creating negative curvature strain. This hypothesis may be tested by measuring key distance constraints in TP-1 when bound to the lipid bilayer and by measuring the depth of insertion of TP-1. Alternatively, the different curvature behaviors of TP-1 and PG-1 may result from the different charge distributions of the two peptides. The cationic residues of TP-1 are located at the N- and C-termini and in the middle of the β -strands, while the Arg residues of PG-1 are clustered to the β -turn at one end of the molecule and the two termini at the other end (Fig. 1). Since we have previously determined that PG-1 is inserted into the lipid bilayer with the β -turn near the membrane surface [23,24], electrostatic repulsion among the three β -turn Arg residues should expand the bilayer surface, inducing positive curvature strain. Without such a cationic β -turn, and with three Arg residues located in the middle of the two strands, TP-1 is likely to expand the hydrophobic part of the membrane instead, thus creating a negative curvature strain.

The second surprising result of this study is the similar membrane disruptive ability of TPY4 and TPA4 towards the two anionic bilayers and the stronger perturbation of PC/PG bilayers by the mutants than by the wild-type TP-1 (Figs. 6 and 7). Antimicrobial assays of tachyplesin derivatives showed that TPY4 is similarly effective at inhibiting bacterial and fungal growths as TP-1 while TPA4 is inactive [17]. Thus, one would expect less membrane disorder by TPA4 than by TPY4. The fact that TPY4 and TPA4 cause similar membrane disorder in the two anionic bilayers indicates that membrane disruption is not strongly correlated with antimicrobial activity for the tachyplesin peptides. This complexity has also been noted in previous studies of tachyplesins. For example, measurements of carboxyfluorescein leakage from acidic PC/PA liposomes indicate

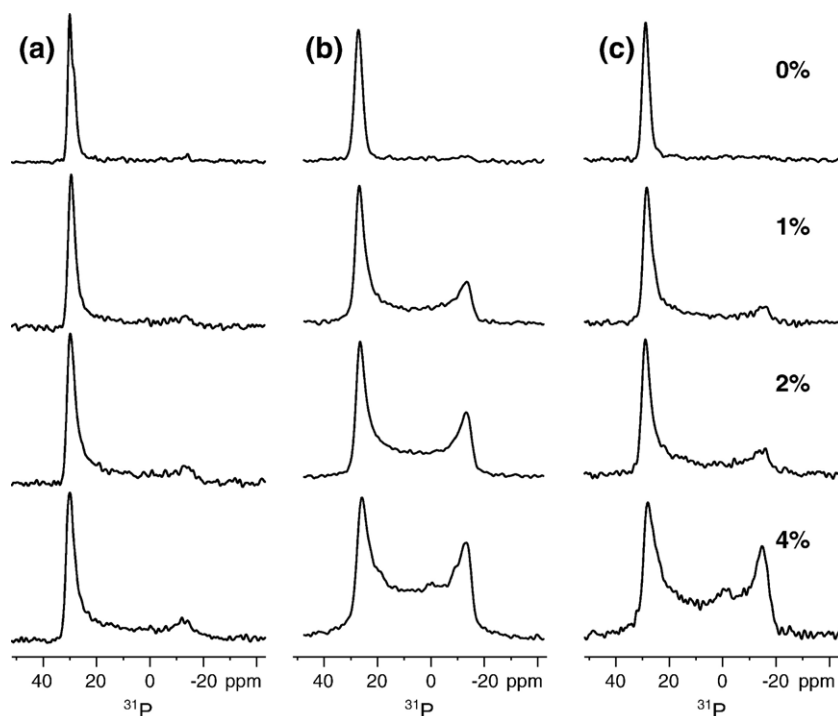


Fig. 7. ^{31}P spectra of uniaxially aligned POPC : POPG (3:1) bilayers in the presence of TP-1 and its linear derivatives. (a) TP-1. (b) TPY4. (c) TPA4. Peptide concentrations are 0, 1%, 2%, and 4%.

that the inactive TPA4 causes similar membrane permeabilization as the active TPY4 and TP-1 [17]. FTIR measurements of TP-Acm, where the SH groups of Cys residues were protected with acetamidomethyl groups, showed that TP-Acm creates larger acyl-chain disorder than TP-1 in PG lipids despite having much weaker membrane permeabilization and micellization abilities than TP-1 [21]. Based on these observations, Matsuzaki and coworkers suggested that tachyplesin peptides interact with lipid membranes with multiple mechanisms: the disulfide-linked TP-1 permeabilizes acidic bilayers at low peptide–lipid molar ratios without causing membrane disorder and achieves this by forming anion-selective pores followed by translocation [22]. In contrast, the linear TP-Acm does not permeabilize acidic membranes except at very high concentrations but disrupts the bilayer organization. Our ^{31}P NMR spectra indicate that TPA4 resembles TP-Acm in being membrane destabilizing without having strong antimicrobial activities while TPY4 possesses both membrane perturbing and antimicrobial activities. These observations imply that membrane permeabilization, which requires pore formation, is a more direct indicator of antimicrobial activity than membrane perturbation for the tachyplesin peptides.

In summary, ^{31}P and ^2H NMR spectra of uniaxially aligned membranes of varying compositions indicate that TP-1 selectively micellizes and randomizes POPE/POPG bilayers but retains the orientational order of neutral and POPC/POPG bilayers. This suggests that TP-1 induces negative curvature strain to the bilayer, which may result from its weaker conformational amphipathicity compared to PG-1. The removal of disulfide bonds in TP-1 abolishes the micellization ability but retains the random orientation distribution of PE/PG and PC/PG anionic bilayers, indicating that the linear tachyplesin derivatives perturb the lipid bilayer organization with a different mechanism from the disulfide-linked TP-1. Therefore, care must be taken in correlating the membrane-perturbing abilities of tachyplesin peptides with their antimicrobial activities.

Acknowledgements

The authors thank Professor A. Andreotti and Dr. A.G. Rao for providing the crude TPY4 and TPA4 peptides and R. Mani for experimental assistance. This work is supported by the National Institutes of Health grant GM-066976 to M. Hong and grants AI-22839 and AI-37945 to A.J. Waring.

References

- [1] I.C.P. Smith, I.H. Ekiel, in: I.C. Gorenstein (Ed.), *Phosphorus-31 NMR: Principles and Applications*, Academic Press, Inc., 1984, pp. 447–475.
- [2] E.J. Prenner, R.N.L.R.N., K.C. Neuman, S.M. Gruner, L.H. Kondejewski, R.S. Hodges, R.N. McElhane, Nonlamellar phases induced by the interaction of gramicidin S with lipid bilayers. A possible relationship to membrane-disrupting activity, *Biochemistry* 36 (1997) 7906–7916.
- [3] B.B. Boney, R.J. Gilbert, P.W. Andrew, O. Byron, A. Watts, Structural analysis of the protein/lipid complexes associated with pore formation by the bacterial toxin pneumolysin, *J. Biol. Chem.* 276 (2001) 5714–5719.
- [4] E. Strandberg, A.S. Ulrich, NMR methods for studying membrane-active antimicrobial peptides, *Concepts Magn. Reson.* 23 (2004) 89–120.
- [5] B. Bechinger, The structure, dynamics, and orientation of antimicrobial peptides in membranes by multidimensional solid-state NMR spectroscopy, *Biochim. Biophys. Acta* 1462 (1999) 157–183.
- [6] J.J. Buffy, M.J. McCormick, S. Wi, A. Waring, R.I. Lehrer, M. Hong, Solid-state NMR investigation of the selective perturbation of lipid bilayers by the cyclic antimicrobial peptide RTD-1, *Biochemistry* 43 (2004) 9800–9812.
- [7] S. Yamaguchi, T. Hong, A. Waring, R.I. Lehrer, M. Hong, Solid-state NMR investigations of peptide–lipid interaction and orientation of a beta-sheet antimicrobial peptide, protegrin, *Biochemistry* 41 (2002) 9852–9862.
- [8] K.A. Henzler Wildman, D.K. Lee, A. Ramamoorthy, Mechanism of lipid bilayer disruption by the human antimicrobial peptide, LL-37, *Biochemistry* 42 (2003) 6545–6558.
- [9] M.S. Balla, J.H. Bowie, F. Separovic, Solid-state NMR study of antimicrobial peptides from Australian frogs in phospholipid membranes, *Eur. Biophys. J.* 33 (2004) 109–116.
- [10] L. Bellm, R.I. Lehrer, T. Ganz, Protegrins: new antibiotics of mammalian origin, *Expert Opin. Investig. Drugs* 9 (2000) 1731–1742.
- [11] T. Nakamura, H. Furunaka, T.M.T., F. Tokunaga, T. Muta, S. Iwanaga, M. Niwa, T. Takao, Y. Shimonishi, Tachyplesin, a class of antimicrobial peptide from the hemocytes of the horseshoe crab (*Tachyplesus tridentatus*). Isolation and chemical structure, *J. Biol. Chem.* 263 (1988) 16709–16713.
- [12] R.L. Fahmer, T. Dieckmann, S.S. Harwig, R.I. Lehrer, D. Eisenberg, J. Feigon, Solution structure of protegrin-1, a broad-spectrum antimicrobial peptide from porcine leukocytes, *Chem. Biol.* 3 (1996) 543–550.
- [13] K. Kawano, T. Yoneya, T. Miyata, K. Yoshikawa, F. Tokunaga, Y. Terada, S. Iwanaga, Antimicrobial peptide, tachyplesin I, isolated from hemocytes of the horseshoe crab (*Tachyplesus tridentatus*). NMR determination of the beta-sheet structure, *J. Biol. Chem.* 265 (1990) 15365–15367.
- [14] A. Laederach, A.H. Andreotti, D.B. Fulton, Solution and micelle-bound structures of tachyplesin I and its active aromatic linear derivatives, *Biochemistry* 41 (2002) 12359–12368.
- [15] R. Mani, A.J. Waring, R.I. Lehrer, M. Hong, Membrane-disruptive abilities of β -hairpin antimicrobial peptides correlate with conformation and activity: A ^{31}P and ^1H NMR study, *Biochim. Biophys. Acta* 1716 (2005) 11–18.
- [16] J. Chen, T.J. Falla, H. Liu, M.A. Hurst, C.A. Fujii, D.A. Mosca, J.R. Embree, D.J. Loury, P.A. Radel, C.C. Chang, L. Gu, J.C. Fiddes, Development of protegrins for the treatment and prevention of oral mucositis: structure–activity relationships of synthetic protegrin analogues, *Biopolymers* 55 (2000) 88–98.
- [17] A.G. Rao, Conformation and antimicrobial activity of linear derivatives of tachyplesin lacking disulfide bonds, *Arch. Biochem. Biophys.* 361 (1999) 127–134.
- [18] K.J. Hallock, K. Henzler Wildman, D.K. Lee, A. Ramamoorthy, An innovative procedure using a sublimable solid to align lipid bilayers for solid-state NMR studies, *Biophys. J.* 82 (2002) 2499–2503.
- [19] R. Mani, J.J. Buffy, A.J. Waring, R.I. Lehrer, M. Hong, Solid-state NMR investigation of the selective disruption of lipid membranes by protegrin-1, *Biochemistry* 43 (2004) 13839–13848.
- [20] C. Ratledge, S.G. Wilkinson, *Microbial Lipids*, vol. 1, Academic Press, London, 1988.
- [21] K. Matsuzaki, M. Nakayama, M. Fukui, A. Otaka, S. Funakoshi, N. Fujii, K. Bessho, K. Miyajima, Role of disulfide linkages in tachyplesin–lipid interactions, *Biochemistry* 32 (1993) 11704–11710.
- [22] K. Matsuzaki, S. Yoneyama, N. Fujii, K. Miyajima, K. Yamada, Y. Kirino, K. Anzai, Membrane permeabilization mechanisms of a cyclic antimicrobial peptide, tachyplesin I, and its linear analog, *Biochemistry* 36 (1997) 9799–9806.
- [23] J.J. Buffy, T. Hong, S. Yamaguchi, A. Waring, R.I. Lehrer, M. Hong, Solid-state NMR investigation of the depth of insertion of protegrin-1 in lipid bilayers using paramagnetic Mn^{2+} , *Biophys. J.* 85 (2003) 2363–2373.
- [24] J.J. Buffy, A.J. Waring, R.I. Lehrer, M. Hong, Immobilization and aggregation of antimicrobial peptide protegrin in lipid bilayers investigated by solid-state NMR, *Biochemistry* 42 (2003) 13725–13734.